Data-driven Modeling and Adaptive Predictive Anti-swing Control of Overhead Cranes

Gyoung-Hahn Kim, Mahnjung Yoon, Jae Young Jeon, and Keum-Shik Hong*

International Journal of Control, Automation, and Systems 20(8) (2022) 2712-2723

ISSN:1598-6446 (print version)
eISSN:2005-4092 (electronic version)

To link to this article:
http://dx.doi.org/10.1007/s12555-022-0025-8

Springer

International Journal of Control, Automation, and Systems 20(8) (2022) 2712-2723
http://dx.doi.org/10.1007/s12555-022-0025-8
ISSN:1598-6446 eISSN:2005-4092
http://www.springer.com/12555

Data-driven Modeling and Adaptive Predictive Anti-swing Control of Overhead Cranes

Gyoung-Hahn Kim, Mahnjung Yoon, Jae Young Jeon, and Keum-Shik Hong*

Abstract: This study investigates a novel data-driven model and an adaptive predictive anti-swing control law for overhead cranes. As an alternative solution to the physics-based modeling approach, a data-driven modeling framework is formulated using the feedforward neural network and extreme learning machine, approximating the nonlinear functional mapping between the system inputs and outputs. Using the proposed data-driven modeling approach, the complete input-output behavior, including the dynamics associated with sensors and actuators, is captured from experimental data. After converting the data-driven model to a state-space form, an adaptive predictive anti-swing control law is developed using the empirical model. To compensate for the modeling discrepancy resulting from abrupt parameter variations, an online parameter adaptation law for updating the data-driven model is further developed. Thus, accurate bridge/trolley positioning and rapid swing suppression are realized in ordinary and uncertain operating conditions. The asymptotic stability of the error dynamics and the boundedness in the estimated parameters are analyzed using the Lyapunov technique. Finally, three types of experiments are performed to verify the effectiveness of the proposed modeling and control methods.

Keywords: Adaptive control, anti-sway control, crane control, data-driven modeling, overhead crane.

1. INTRODUCTION

This paper discusses an anti-sway control problem of an overhead crane (commonly called a bridge crane, see Fig. 1). The overhead crane, which consists of a traveling bridge spanning the gap and a lifting component, is widely utilized to move steel ladles and other metals from one location to another. To improve the crane productivity, the heavy load suspended by the multi-wire hoisting system is required to be transferred in a quick manner. However, the quick manipulation of the crane can generate large payload swings, causing a serious safety issue. Additionally, the unwanted load oscillations at the target position certainly incur unfavorable delays during crane operations. Therefore, this paper aims to develop an appropriate control strategy for suppressing the payload swings at the target position, which consequently solves the important technical issue limiting the operational efficiency of the overhead crane.

Various anti-swing control methods for industrial cranes have been extensively studied over the past decades [1–20]. Among the different types of control schemes, the most typical approach, which has been widely adopted in practical applications, is to plan the optimal trajectories of the trolley by minimizing the residual swing of the load at the target position. Such trajectory planning can be achieved by thoroughly analyzing the relation between the trolley motion and the payload swing [1,2]. The

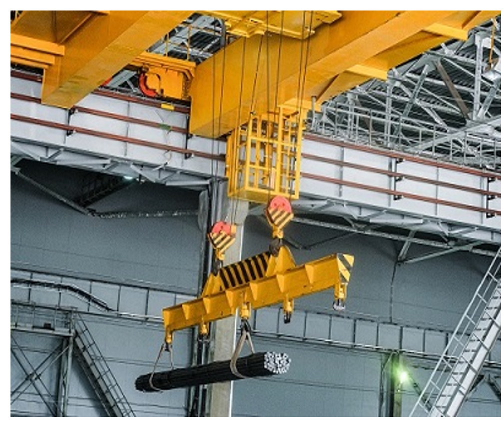

Fig. 1. Overhead crane (https://weeklysafety.com/blog/overhead-cranes).

Manuscript received January 10, 2022; revised March 27, 2022; accepted May 23, 2022. Recommended by Editor Kyoung Kwan Ahn. This work was supported in part by the 2021 Post-Doc Development Program of Pusan National University and in part by the Korea Institute of Energy Technology Evaluation and Planning (KETEP) under the Ministry of Trade, Industry and Energy, Korea (grant no. KETEP-20213030020160).

Gyoung-Hahn Kim and Keum-Shik Hong are with the School of Mechanical Engineering, Pusan National University, Busan 46241, Korea (e-mails: {hahn, kshong}@pusan.ac.kr). Mahnjung Yoon and Jae Young Jeon are with the POWER MnC Co., Ltd., Ulsan 44988, Korea (e-mails: {ymj, jjy}@powermnc.com).
* Corresponding author.

input-shaping control is an open-loop control method in which a series of shaped command profiles are generated to move the trolley while assuring the minimal payload sway [3–6]. Partial feedback linearization control is used to establish a simplified closed-loop control system using coupling effects [7,8]. Sliding-mode control is strongly preferred to enhance the robustness of the crane system against parameter uncertainties [9–11]. Additionally, as an advanced method, adaptive control methods have been adopted for industrial crane systems [12,13]. Passivity-based control schemes are recommended when accurate kinetic and potential energies can be derived [14,15]. Recently, control problems of cranes with input nonlinearities have attracted significant attention, for example, input saturation [16] and input dead-zone [17]. Moreover, several other control methods have been successfully applied to crane systems for the sway suppression of the payload, which include delayed feedback control [18], boundary control [19], and intelligent control [20].

Basically, the dynamic models of overhead cranes can be developed using two approaches, that is, a physics-based approach (i.e., Newton's law or the Lagrange equation) and a data-driven approach (an empirical model). In the existing works, the physics-based crane models were widely adopted for control system design. This is because the physics-based approach is known to be extremely useful in terms of analyzing the controller with insight regarding the underlying physics, particularly when designing a prototype controller for the first time. Therefore, up to now, the control problems of various overhead cranes have been addressed using physics-based models [21–27]. For instance, the modeling and control problem of a three-dimensional (3D) crane was discussed in [21]. In the case that the payload is very large and therefore the distance from the hook to the payload cannot be neglected, a double-pendulum effect should be considered in the control system. For this issue, in [22], the enhanced-coupling adaptive control was developed in consideration of the double-pendulum swing model. In [23], the modeling and vibration control of a flexible overhead crane bridge was discussed by investigating the deflection of the main beam of the gantry crane under the load. To deliver the large/heavy cargo cooperatively using two overhead cranes, a new mathematical model and nonlinear anti-swing control were proposed in [24]. Because the working environments are usually complex, the emergency braking problem has become an important issue for overhead crane applications. To ensure safety and avoid an accident such as collisions, the control problem of simultaneous payload swing suppression and trolley braking was solved in [25]. To avoid serious product damage in constrained operating conditions, the model predictive control was developed in [26]. Concerning the measurement system of the overhead crane, the use of visual tracking technology rather than physical encoders was introduced in [27].

Although the existing control methods for overhead crane systems are workable, the following issues and aspects need to be further improved. i) Due to the underactuated property of the crane system (i.e., the degrees of freedom of the system are larger than the number of control inputs), most existing methods need a model transformation technique enabling the effective coupling between the actuated motion (i.e., the trolley motion) and the unactuated motion (i.e., the swing motion). For this issue, knowledge of the underlying physics is inevitably required in the control formulation. ii) A lot of time and effort is typically required to find out reliable parameters in the mathematical model, which can describe the complex dynamic behavior of the overhead crane systems well. Also, the model tuning process in consideration of the modeling uncertainties and input nonlinearities stemming from the complex mechanical structures and electrical components becomes another task.

To address the aforementioned issues regarding physics-based modeling and its controller design, one of the promising alternatives is a data-driven approach, which involves determining the model structure and parameters using experimental data. However, until now, data-driven modeling and anti-swing control problem has not been studied in the literature. One of the main reasons lies in the fact that it is difficult to obtain a simple structure to facilitate the control design process while guaranteeing high prediction accuracy for nonlinear underactuated overhead crane systems. Therefore, the lack of data-driven modeling and anti-swing control for the overhead crane greatly motivates this research.

This paper investigates the data-driven modeling and adaptive predictive anti-swing control method of overhead cranes. First, using the input and output data acquired from the appropriate excitation signal, the neural network-based data-driven model with the extreme learning machine is established. Then, with the data-driven model converted into the state-space form, an adaptive predictive anti-swing control is formulated using online model learning. Finally, extensive experimental results obtained from the scale-down overhead crane are provided to validate the effectiveness of the proposed modeling and control scheme.

Because the overhead crane system is a typical underactuated mechanical system, the data-driven modeling and control method developed in this study can be applied to various underactuated mechanical systems exhibiting similar dynamic properties. In other words, provided that informative data can be obtained for the considered underatuated systems, the mathematical modeling, and the subsequent control design can be performed in a similar manner without thorough background knowledge of the underlying physics. Furthermore, the proposed modeling and control scheme can be extended to deal with the challenging control problems such as the state-constrained control problem by establishing the constrained optimization problem in the proposed control formulation [28,29]. Therefore, the results in this paper have values in both theory and practice.

The contributions of this paper are summarized as follows: i) As an alternative model to the physics-based crane dynamic modeling, a novel data-driven modeling approach is proposed using the feedforward neural networks. In contrast to the physics-based method, the proposed modeling method does not require unrealistic assumptions (i.e., mass-less rod, no friction, etc.) about the system behavior. Moreover, the complete input-output behavior including the dynamics associated with sensors and actuators are captured in the experimental data. Consequently, the time-consuming effort on the model validation can be saved. ii) A new adaptive predictive anti-swing control is developed by means of the proposed data-driven model. By introducing the online parameter adaptation law, the data-driven model is updated to compensate for the model discrepancy resulting from the abrupt parameter variations, which cannot be considered in the offline data-driven modeling process. Therefore, the proposed anti-swing control method based on the data-driven model is very effective for both ordinary and uncertain operating conditions.

The remainder of this paper is organized as follows: In Section 2, the data-driven model of the overhead crane system is developed. In Section 3, the adaptive predictive anti-swing control is designed based on the data-driven model. The experimental results are provided in Section 4. Conclusions are given in Section 5.

2. DATA-DRIVEN MODELING

Fig. 2 shows a schematic of the typical overhead crane system. Here, **XYZ** denotes the fixed coordinate system and $X_tY_tZ_t$ denotes the trolley coordinate system that moves along with the trolley. The bridge girder spanning two runway beams moves along the X_t (travel) direction, and the trolley moves on the girder in the Y_t (traverse) direction. Based on the coordinate systems, the position of the trolley system is defined as $(x, y, 0)$. In addition, δ and θ are the swing angles, which indicate the rotational angles of the load along the X_t and Y_t-axis in the trolley coordinate system, respectively. On the crane dynamics, because the system inputs (i.e., trolley driving forces) and the system outputs (i.e., system state information) are available through the measurement systems, the data-driven modeling scheme can be realized. Considering that the crane system is a highly nonlinear and underactuated dynamic system, the nonlinear autoregressive form with an exogenous input (NARX) is adopted in this study for the data-driven modeling

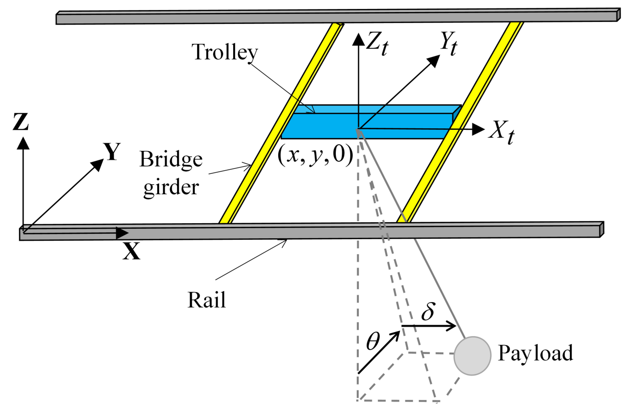

Fig. 2. Schematic of a overhead bridge crane.

$$y(k+1) = f_{\text{NARX}}(u(k),\ u(k-1),\ \cdots,\ u(k-n_u+1),\ y(k),\ y(k-1),\ \cdots,\ y(k-n_y+1)), \quad (1)$$

where $u(k) \in \mathbb{R}^m$ and $y(k) \in \mathbb{R}^n$ are the system inputs and outputs, respectively; n_u and n_y represent the number of past input and output samples respectively; m and n indicate the dimensions of the inputs and outputs, respectively. In (1), the augmented input vector can be defined as follows:

$$\begin{aligned}\underline{x}(k) = [&u(k),\ u(k-1),\ \cdots,\ u(k-n_u+1),\\ &y(k),\ y(k-1),\ \cdots,\ y(k-n_y+1)]^T\\ \in\ &\mathbb{R}^{\tilde{n}=mn_u+nn_y}.\end{aligned} \quad (2)$$

The measurement sequence of the crane system can then be converted into the form of N arbitrary distinct samples, which is given as

$$\{(\underline{x}_1,\ y_1),\ \cdots,\ (\underline{x}_N,\ y_N)\} \in (\chi,\ \xi), \quad (3)$$

where $\chi \in \mathbb{R}^{\tilde{n}=mn_u+nn_y}$ and $\xi \in \mathbb{R}^n$.

In the context of the nonlinear system identification, the above sample form is used to approximate the nonlinear function mapping in (1), and the future output of the system can be predicted by means of the identified model. In this study, in order to develop the data-driven model of the overhead crane in an effective manner, the generalized single-hidden layer feedforward networks (SLFNSs) with $\tilde{N}$ number of hidden nodes and activation function $g(x)$ (typically a sigmoidal function) is introduced for the unknown function approximation. This is mathematically given as follows:

$$\begin{aligned}\hat{x}(k+1) = \hat{y}(k+1) &= f_{\text{DATA}}(\underline{x}(k))\\ &= \sum_{i=1}^{\tilde{N}} \beta_i g(w_i \cdot \underline{x}(k) + b_i),\end{aligned} \quad (4)$$

where $w_i = [w_{i1},\ w_{i2},\ \cdots,\ w_{i\tilde{n}}]^T$ is the weight vector connecting the ith hidden node and the input nodes, $\beta_i = [\beta_{i1},\ \beta_{i2},\ \cdots,\ \beta_{in}]^T$ is the weight vector connecting the ith hidden node and the output nodes, and b_i is the threshold of the ith hidden node. $w_i \cdot \underline{x}_j$ denotes the inner product of w_i and $\underline{x}_j$. The data-driven model in (4) can be rewritten in a compact form, which is given as follows:

$$\hat{x}(k+1) = W^T g(W_r^T \underline{x}(k) + b_r), \tag{5}$$

where

$$W_r = \begin{bmatrix} w_{11} & w_{12} & \cdots & w_{1\tilde{n}} \\ w_{21} & w_{22} & & w_{2\tilde{n}} \\ \vdots & & \ddots & \vdots \\ w_{\tilde{N}1} & w_{\tilde{N}2} & \cdots & w_{\tilde{N}\tilde{n}} \end{bmatrix}^T, \; b_r = \begin{bmatrix} b_1 \\ b_2 \\ \vdots \\ b_{\tilde{N}} \end{bmatrix},$$

$$W = \begin{bmatrix} \beta_{11} & \beta_{12} & \cdots & \beta_{1n} \\ \beta_{21} & \beta_{22} & & \beta_{2n} \\ \vdots & & \ddots & \vdots \\ \beta_{\tilde{N}1} & \beta_{\tilde{N}2} & \cdots & \beta_{\tilde{N}n} \end{bmatrix}.$$

It should be noted that input weights of W_r are chosen at random and output weight matrix W is determined analytically using Moore-Penrose generalized inverse (see [30,31] for more details). Consequently, the neural network in (5), which is optimized by the algorithm called the extreme learning machine, can work as a universal approximator for the unknown crane dynamics.

To facilitate the control design, the mathematical model given in (5) is transformed into a state-space form using neural network linearization. Because the nonlinear mapping function in (4) satisfies the continuously differentiable and globally Lipschitz condition, the data-driven model can be linearized around any operating point $\underline{x}_0$ (particularly, the equilibrium point). The Jacobian matrix $\partial f_{\mathrm{DATA}}/\partial \underline{x}$ can be obtained as follows:

$$\left.\frac{\partial f_{\mathrm{DATA}}}{\partial \underline{x}}\right|_{\underline{x}=\underline{x}_0} = \Upsilon W^T \left.\frac{\partial g}{\partial \underline{x}}\right|_{\underline{x}=\underline{x}_0}, \tag{6}$$

where

$$\Upsilon = \mathrm{diag}\{(x_{\max,1} - x_{\min,1})/2, \; \cdots, \; (x_{\max,n} - x_{\min,n})/2\},$$

$$\left.\frac{\partial g}{\partial \underline{x}}\right|_{\underline{x}=\underline{x}_0} = \begin{bmatrix} \partial g_1/\partial \underline{x}_1 & \partial g_1/\partial \underline{x}_2 & \cdots & \partial g_1/\partial \underline{x}_{\tilde{n}} \\ \partial g_2/\partial \underline{x}_1 & \partial g_2/\partial \underline{x}_2 & & \partial g_2/\partial \underline{x}_{\tilde{n}} \\ \vdots & & \ddots & \vdots \\ \partial g_{\tilde{N}}/\partial \underline{x}_1 & \partial g_{\tilde{N}}/\partial \underline{x}_2 & \cdots & \partial g_{\tilde{N}}/\partial \underline{x}_{\tilde{n}} \end{bmatrix}_{\underline{x}=\underline{x}_0},$$

$$\frac{\partial g_i}{\partial \underline{x}_j} = \frac{2W_r(j,i)\Omega}{(\underline{x}_{\max,j} - \underline{x}_{\min,j})(1+\Omega)^2},$$

$$\Omega = e^{-\left\{W_{r,i}{}^T [2((\underline{x}-\underline{x}_{\min})/(\underline{x}_{\max}-\underline{x}_{\min}))-\mathbf{1}] + b_{r,i}\right\}},$$

where $W_{r,i}$ indicates the ith column of W_r and $b_{r,i}$ represents the ith elements of b_r and $\underline{x}_j$ indicates the jth elements of $\underline{x}$ and $W_r(j,i)$ denotes the entry in the jth row ith column of W_r.

In this study, by assuming that the state variables of the crane system (i.e., displacement, velocity, swing angle, and angular velocity) are measurable, the input and state vectors at time k are considered as $u(k) = [u_x \;\; u_y]^T$ and $x(k) = [x \;\; v_x \;\; y \;\; v_y \;\; \delta \;\; v_\delta \;\; \theta \;\; v_\theta]^T$ for n_u, $n_y = 1$. Then, the one-step-ahead prediction model of the overhead crane in a discrete-time state-space form can be obtained as follows:

$$\begin{aligned} x(k+1) &= A_{\mathrm{DATA}} x(k) + B_{\mathrm{DATA}} u(k), \\ y(k) &= Cx(k), \end{aligned} \tag{7}$$

where $C = I_{8\times 8}$ and the data-driven system matrices $A_{\mathrm{DATA}} \in \mathbb{R}^{8\times 8}$ and $B_{\mathrm{DATA}} \in \mathbb{R}^{8\times 2}$ are derived by partitioning the Jacobian matrix as follows:

$$\left[\left.\frac{\partial f_{\mathrm{DATA}}}{\partial \underline{x}}\right|_{\underline{x}=\underline{x}_0}\right]_{8\times 10} = [B_{8\times 2} | A_{8\times 8}]. \tag{8}$$

Remark 1: The equilibrium state means that the crane system is at a stable configuration, that is, the velocities of the trolley and bridge girder, together with swing angle and angular velocity, are all zero, no matter where the trolley and bridge are located. This condition is reasonable and fits the actual property of crane systems [26]. Therefore, the equilibrium state in (6) is defined as $\underline{x}_0 = [0 \;\; 0 \;\; x_0 \;\; 0 \;\; y_0 \;\; 0 \;\; 0 \;\; 0 \;\; 0 \;\; 0]^T$, in which x_0 and y_0 are the initial positions of the trolley and bridge girder, respectively.

3. ADAPTIVE PREDICTIVE ANTI-SWING CONTROL

In this section, an adaptive predictive anti-swing control will be designed. The design objective is to find the optimal future control actions, which transport the payload to the desired position with minimal residual vibrations. To begin with the proposed control design, let us consider the performance index function given as follows:

$$J = (Y - Y^*)^T \tilde{Q} (Y - Y^*) + U^T \tilde{R} U, \tag{9}$$

where $Y = [y(k+1), y(k+2), \cdots, y(k+N_p)]^T$ is the future output matrix, $Y^* = [y^*(k+1), y^*(k+2), \cdots, y^*(k+N_p)]^T$ is the desired future output, $U = [u(k+1), \cdots, u(k+N_c)]^T$ is the future input matrix, N_p is the size of the predictive horizon, N_c is the size of the control horizon satisfying $N_c \le N_p$, $\tilde{Q} = \mathrm{diag}(Q_{8\times 8}, \cdots, Q_{8\times 8}) \in \mathbb{R}^{8N_p \times 8N_p}$ is the weighting matrix for tracking errors between the predicted output and the set-point signal, and $\tilde{R} = \mathrm{diag}(R_{2\times 2}, \cdots, R_{2\times 2}) \in \mathbb{R}^{2N_c \times 2N_c}$ is the control weighting matrix. Using the obtained data-driven model in (7), the future output $y(k+i)$, $i = 1, \cdots, N_p$ in (9) can be further described as follows:

$$\begin{cases} y(k+1) = CA_{\mathrm{DATA}} x(k) + CB_{\mathrm{DATA}} u(k), \\ y(k+2) = CA_{\mathrm{DATA}}^2 x(k) + CA_{\mathrm{DATA}} B_{\mathrm{DATA}} u(k) \\ \qquad\qquad + CB_{\mathrm{DATA}} u(k+1), \end{cases}$$

$$
\begin{cases}
y(k+3) = CA_{\mathrm{DATA}}^3 x(k) + CA_{\mathrm{DATA}}^2 B_{\mathrm{DATA}} u(k) \\
\qquad + CA_{\mathrm{DATA}} B_{\mathrm{DATA}} u(k+1) \\
\qquad + CB_{\mathrm{DATA}} u(k+2), \\
\qquad \vdots \\
y(k+N_p) = CA_{\mathrm{DATA}}^{N_p} x(k) + CA_{\mathrm{DATA}}^{N_p-1} B_{\mathrm{DATA}} u(k) \\
\qquad + CA_{\mathrm{DATA}}^{N_p-2} B_{\mathrm{DATA}} u(k+1) + \cdots \\
\qquad + CA_{\mathrm{DATA}}^{N_p-N_c} B_{\mathrm{DATA}} u(k+N_c-1).
\end{cases}
\tag{10}
$$

To facilitate the controller design process, (10) can be rewritten in the following compact matrix form.

$$Y = Fx(k) + \Phi U, \tag{11}$$

where $F = [CA_{\mathrm{DATA}}, CA_{\mathrm{DATA}}^2, \cdots, CA_{\mathrm{DATA}}^{N_p}]^T$, and

$$
\Phi = \begin{bmatrix}
CB_{\mathrm{DATA}} & 0 & 0 & \cdots & 0 \\
CA_{\mathrm{DATA}} B_{\mathrm{DATA}} & CB_{\mathrm{DATA}} & 0 & \cdots & 0 \\
CA_{\mathrm{DATA}}^2 B_{\mathrm{DATA}} & CA_{\mathrm{DATA}} B_{\mathrm{DATA}} & CB_{\mathrm{DATA}} & \cdots & 0 \\
\vdots & & \vdots & & \vdots \\
CA_{\mathrm{DATA}}^{N_p-1} B_{\mathrm{DATA}} & CA_{\mathrm{DATA}}^{N_p-2} B_{\mathrm{DATA}} & CA_{\mathrm{DATA}}^{N_p-3} B_{\mathrm{DATA}} & \cdots & CA_{\mathrm{DATA}}^{N_p-N_c} B_{\mathrm{DATA}}
\end{bmatrix}.
$$

Then, by substituting (11) into (9), and after some simplification, we obtain the following simplified cost function

$$J = U^T(\Phi^T \tilde{Q} \Phi + \tilde{R})U + 2U^T \Phi^T \tilde{Q} F e(k). \tag{12}$$

To drive the state of the system to the desired state, the controller is designed by minimizing the above index function. Let $\partial J / \partial U = 0$. The solution becomes

$$U = -(\Phi^T \tilde{Q} \Phi + \tilde{R})^{-1} \Phi^T \tilde{Q} F e(k). \tag{13}$$

Now, the system control input at the present time instant k is obtained as

$$u(k) = K^T U, \tag{14}$$

where $K \in \mathbb{R}^{2N_c \times 2}$ represents the auxiliary vector with the following expression.

$$K = [I_{2\times 2}\ 0_{2\times 2}\ \cdots\ 0_{2\times 2}]^T.$$

When the next sample period arrives, the more recent measurement is taken to form (10) for calculating the new sequence of the control signal in (13). By repeating these steps, the payload can be transported to the final position with minimal swings.

Remark 2: The control law in (13) corresponds to the state feedback control within the framework of predictive control. Therefore, the prediction accuracy of the data-driven model is important for achieving the satisfactory control performance. Under the conditions of persistent excitation (i.e., plentiful information of the amplitude and frequency within the excitation input signals), the data-driven model is effective to capture the dominant dynamic characteristics of the crane system with the desired degree of prediction accuracy [32,35–37]. However, such persistent excitation cannot be easily guaranteed in practice, and unexpected parameter variations in the crane system can occur during the operation. For this reason, an online parameter adaptation algorithm is developed in this study.

Let $\Xi(k)$ be the instantaneous prediction error for the prediction output $\psi = g(W_r^T \underline{x}(k) + b_r)$ and the real output $y(k)$, the parametric error equation can be obtained as follows:

$$
\begin{aligned}
\Xi(k) &= y(k) - W^T \psi(k) = W^{*T} \psi(k) - W^T \psi(k) \\
&= \tilde{W}^T \psi(k),
\end{aligned}
\tag{15}
$$

where $\tilde{W} = W^* - W$ indicates the parametric error matrix between the true model parameter matrix W^* and the output weight matrix W. Then, the data-driven model obtained offline can be updated by the following law proposed

$$W(k+1) = W(k) + \Gamma_G(\psi(k)\Xi^T(k)), \tag{16}$$

where $\Gamma_G = \mathrm{diag}(\Gamma_{G1}, \cdots, \Gamma_{G\tilde{N}}) \in \mathbb{R}^{\tilde{N} \times \tilde{N}}$ is the update gain matrix for the parameter adaptation algorithm.

Theorem 1: The parameter update law given by (16) guarantees that the estimated output $\hat{y}(k)$ converges to the actual output $y(k)$ and the weight matrix W converges to a constant matrix W^*, respectively. This also guarantees that the online model predictions are bounded as long as the system output is bounded.

Proof: Let us consider the following Lyapunov function candidate

$$V(\tilde{W}) = \mathrm{tr}(\tilde{W}^T \Gamma_G^{-1} \tilde{W}), \tag{17}$$

where tr represents the trace of a matrix. Then, one can obtain the following results.

$$
\begin{aligned}
\Delta V(\tilde{W}) &= V(\tilde{W}(k+1)) - V(\tilde{W}(k)) \\
&= \mathrm{tr}(\tilde{W}^T(k+1) \Gamma_G^{-1} \tilde{W}(k+1)) \\
&\quad - \mathrm{tr}(\tilde{W}^T(k) \Gamma_G^{-1} \tilde{W}(k)) \\
&= \mathrm{tr}(-2\tilde{W}^T(k) \psi(k) \Xi^T(k) \\
&\quad + \Xi(k) \psi^T(k) \Gamma_G \psi(k) \Xi^T(k)) \\
&= \mathrm{tr}(-2\Xi(k)\Xi^T(k) + \Xi(k)\psi^T(k)\Gamma_G \psi(k)\Xi^T(k)) \\
&= -2\Xi^T(k)\Xi(k) + \Xi^T(k)\Xi(k)\psi^T(k)\Gamma_G \psi(k) \\
&= -2\Xi^T(k)\Xi(k) + \Xi^T(k)\psi^T(k)\Gamma_G \psi(k)\Xi(k)
\end{aligned}
$$

$$= -\Xi^T(k)\Lambda\Xi(k), \tag{18}$$

where $\Lambda = 2 - \psi^T(k)\Gamma_G\psi(k)$. Now it can be concluded that $V(k+1) - V(k) \leq 0$ if $\Lambda > 0$ or $0 < \lambda_{\max}(\Gamma_G) < 2$. This implies that $V(\tilde{W}) \geq 0$ is non-increasing, and we have

$$\sum_{k=0}^{\infty}(V(k+1) - V(k)) = -\sum_{k=0}^{\infty}\Xi^T(k)\Lambda\Xi(k)$$
$$\Rightarrow \sum_{k=0}^{\infty}\Xi^T(k)\Lambda\Xi(k) = V(0) - V(\infty) < \infty. \tag{19}$$

Additionally, if $\Lambda > I$ is satisfied

$$\sum_{k=0}^{\infty}\Xi^T(k)\Xi(k) \leq \sum_{k=0}^{\infty}\Xi^T(k)\Lambda\Xi(k) < \infty. \tag{20}$$

Therefore, $\Xi(k) \in \mathcal{L}_2$ and $(W(k+1) - W(k)) \in \mathcal{L}_2 \cap \mathcal{L}_\infty$. Finally, using Barbalat's lemma [33],

$$\begin{cases} \lim_{k\to\infty}\Xi(k) = 0, \\ \lim_{k\to\infty}W(k+1) = W(k). \end{cases} \tag{21}$$

From (21), Theorem 1 is proven. □

As long as the estimated output $\hat{y}(k)$ converges to the actual output $y(k)$ and the system matrices A_{DATA} and B_{DATA} are stabilizable, it is noted that the stability of the closed-loop system with the proposed predictive anti-swing control is ensured by properly setting the control parameters Q and R [34].

Remark 3: The control horizon N_c is chosen to be less than (or equal to) the prediction horizon N_p. With too short prediction and control horizons, the closed-loop predictive control system can become unstable. For the closed-loop stability and desired performance, the tuning parameters Q and R are typically designed such that the closed-loop system $A_{\text{DATA}} - B_{\text{DATA}}K^T(\Phi^T\tilde{Q}\Phi + \tilde{R})^{-1}\Phi^T\tilde{Q}F$ becomes stable. Such tuning parameters also need to be determined such that the condition number $\kappa(\Phi^T\tilde{Q}\Phi + \tilde{R})$ is sufficiently small because the large condition number for a long prediction horizon results in the numerical instability. For tuning the update gain matrix Γ_G in the parameter adaptation algorithm, the condition $0 < \lambda_{\max}(\Gamma_G) < 2$ should be satisfied to guarantee the boundness of the online model predictions. In this paper, based on the aforementioned tuning guideline, the control parameters for the best performance are obtained by trial and error upon several experiments.

In summary, when new data measurements are made during the task, the weight matrix obtained with offline training data is updated first using the adaptation law in (16). Then, after transforming the updated model into the state-space form by applying (6), the predictive anti-swing control law in (13) is recomputed to minimize the $J(e)$ based on the updated data-driven model. This control task is repeated for every new sampling period until the control objective is achieved. Finally, The proposed control method using the adaptation law is summarized in Algorithm 1.

Algorithm 1: Algorithm for the adaptive predictive anti-swing control based on the data-driven model.

Input: The data-driven model in (5) and (7)
Select the initial and target positions of the crane system
1: **While** (Crane positioning and anti-swing uncompleted) **do**
2: The control signal by (14) is sent to the crane
3: The bridge/girder move to the target position
4: **calculate:**
5: The parameter adaptation algorithm by (16)
6: The Jacobian matrix by (6)
7: The updated data-driven model by (7)
8: The control input by (11)-(13)
9: **end calculate**
10: Update the control system
11: **end while**

4. EXPERIMENTS

In this section, a series of experiments were performed to show the effectiveness of the proposed method. As shown in Fig. 3, a scale-downed overhead bridge crane, which is capable of emulating a real overhead crane system, was used to validate the proposed data-driven modeling and control method. The experimental platform was composed of the control part (including the control PC and DAQ board), the actuation part (including DC motors with the motor driver), the measurement part (i.e., encoders), and the mechanical part (mainly composed of a girder, a bridge, and a payload connected to the hoisting rope). The system parameters (i.e., the payload mass m, bridge mass M_x, girder mass M_y, and rope length l) of the self-built overhead crane platform are as follows:

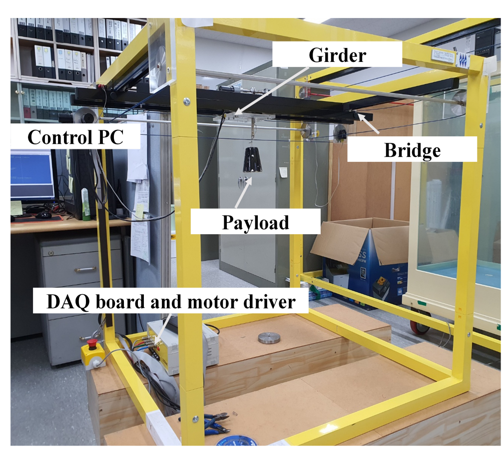

Fig. 3. Experimental testbed.

$$m = 0.73 \text{ kg}, \; M_x = 3 \text{ kg}, \; M_y = 1.72 \text{ kg}, \; l = 0.32 \text{ m}. \tag{22}$$

and the sampling period T_s is 0.05 s.

4.1. Data-driven model development

Owing to the underactuated nature of the crane system, the dynamic behavior of the overhead crane is dominated by the coupling dynamics between trolley movements and payload swings. Thus, the driving force of the trolley is considered as the main control input for both the trolley and bridge dynamics and payload swing dynamics. In the experiment, an amplitude-modulated pseudo-random binary signal (A-PRBS) was chosen as the input to the trolley driving system to construct the data-driven model. This signal was generated from the pseudo-random binary signal (PRBS) by assigning random amplitudes to each step, which is significantly effective to obtain plentiful but not computationally high demanding information about the dominant dynamic characteristics in terms of the nonlinear system identification [35–37]. Therefore, in this study, all data for the model development was obtained by the excitation signal (i.e., A-PRBS) given in Fig. 4.

In developing the data-driven crane dynamics with the proposed modeling method, a SLFNs with 30 hidden neurons was established to capture the underlying physics. All acquired data were normalized to lie between $[-1, +1]$ before determining the output weight matrix. Then, the data-driven model given in (5) and (7) were derived utilizing the normalized input and output data. The one-step ahead output predictions of the developed data-driven models with the input data are given in Fig. 5 by comparing them with the original output data. As can be seen in the results, the complex dynamic behavior of the overhead crane system was well described by the data-driven models with high prediction accuracy. Furthermore, it is

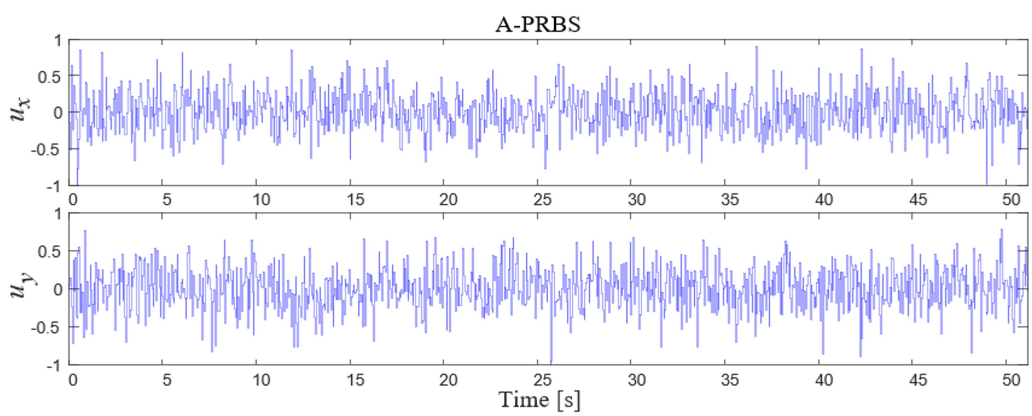

Fig. 4. Input excitation signal for nonlinear system identification (A-PRBS).

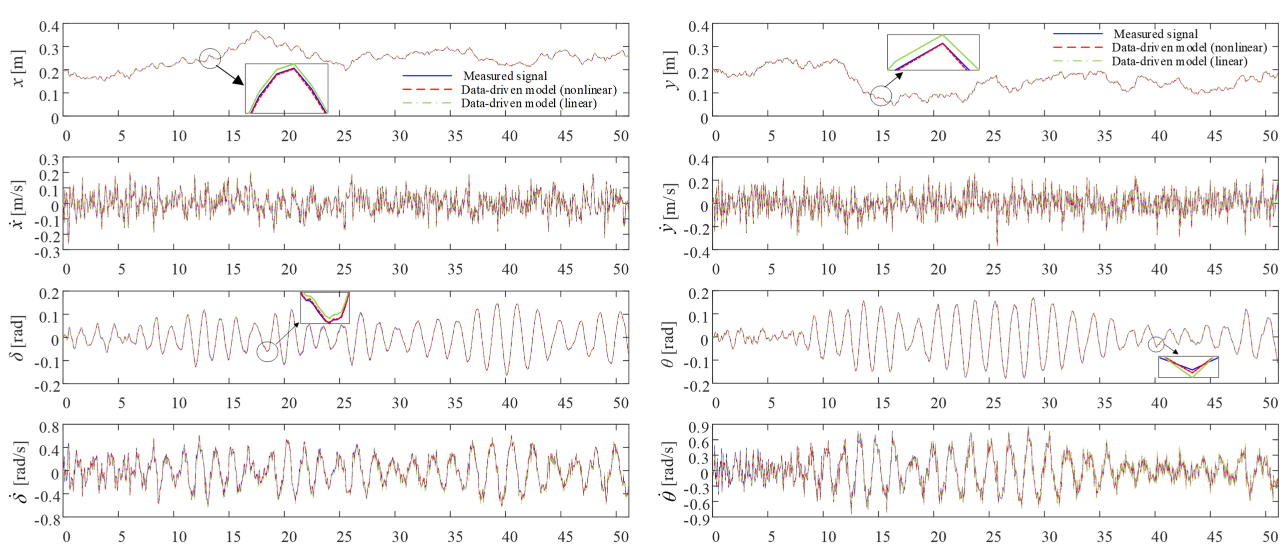

Fig. 5. One-step ahead predictions of the data-driven crane model.

clear that sufficient prediction performance was also guaranteed even after the neural network linearization. Consequently, the experimental results illustrate that the prediction model based on the data-driven modeling approach can be exploited for the control design.

4.2. Control experiments

Using the developed data-driven crane model, a series of control experiments were performed to validate the feasibility and robustness of the proposed adaptive predictive anti-swing control law. The control parameters in the present control scheme were selected as follows:

$$\begin{aligned} &Q = \mathrm{diag}(3,\ 0,\ 4,\ 0,\ 1,\ 0,\ 1,\ 0),\\ &R = 0.01 \times I_{2\times 2},\\ &\Gamma_G = 0.03 \times I_{30\times 30},\\ &N_c = 15,\ N_p = 15, \end{aligned} \tag{23}$$

which were used (i.e., do not require retuning) in all experiments. Then, three groups of experiments were implemented.

Experiment 1: The main purpose of Experiment 1 was to demonstrate the control performance of the predictive anti-swing control law using the obtained data-driven model (without online parameter adaptation). Therefore, the experimental scenario was established in the following two cases:

Case 1 (nominal system parameters)**:** Experimental conditions were set the same as the data-driven model development (i.e., $m = 0.73$ kg and $l = 0.32$ m).

Case 2 (uncertain system parameters)**:** The payload mass 0.73 kg was replaced by the mass of 1.4 kg (approximately 200% increases from its nominal value), and a time-varying rope length (i.e., the hoisting rope was shortened from 0.32 m to 0.15 m) was considered instead of the constant rope length.

The corresponding experimental results are shown in Fig. 6. As shown in Fig. 6(a), when the experimental situations were the same as those of the data-driven modeling, the predictive anti-swing controller could drive the bridge and girder to the target positions within 2 s, with no payload oscillations at the final positions. However, the experimental results given in Fig. 6(b) indicate that the control performance of the predictive controller could be degraded for the case of different experimental conditions (i.e., changed payload mass and time-varying rope length). Particularly, the payload oscillations in the traverse direction were not suppressed by the designed controller, and thus the girder position could not be kept at the target position because the girder, which was lighter weight than that of the bridge, is more affected by the payload swings resulting from the increased moment of inertia. Therefore, it was found from the experimental results that the predictive anti-swing control based on the data-driven crane model was significantly effective for the nominal system, but the prediction anti-swing control required to be adapted online against the abrupt parameter variations which cannot be considered in the offline data-driven modeling.

Experiment 2: The second experiment was performed to demonstrate the effectiveness of the proposed adaptive predictive anti-swing control using the data-driven crane model. For the comparative results to Experiment 1, the proposed controller was implemented for the same un-

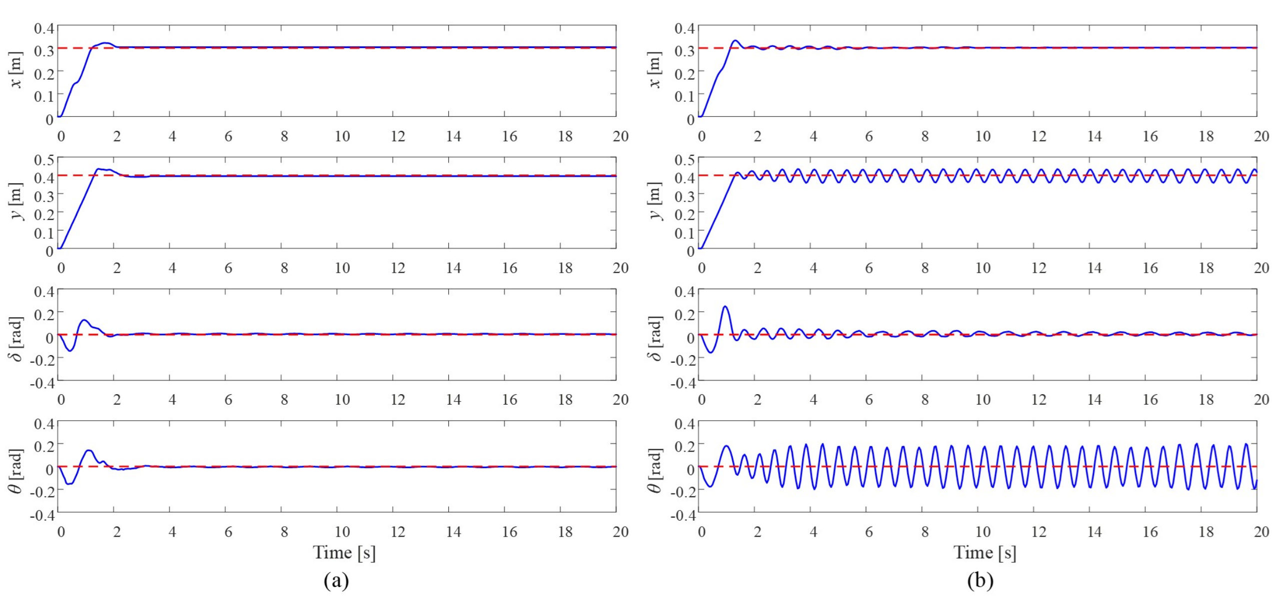

Fig. 6. Experiment 1 – Predictive anti-swing control without online parameter adaptation: (a) nominal system parameters (Case 1) and (b) uncertain system parameters (Case 2).

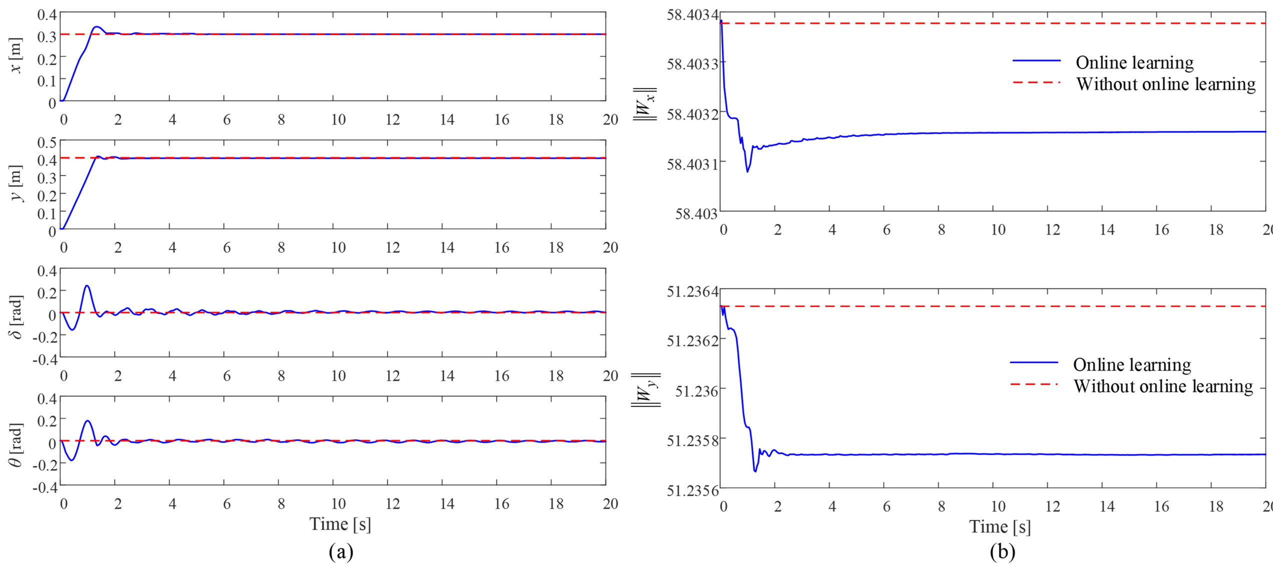

Fig. 7. Experiment 2 – Proposed adaptive predictive anti-swing control against the parameter uncertainties: (a) crane responses and (b) online parameter estimation.

certain parameter conditions (i.e., changed payload mass and time-varying rope length). The experimental data are given in Fig. 7(a). As compared to Fig. 6(b), it is not difficult to find that the satisfactory control performance has been achieved, which indicates that the proposed method has good robustness in terms of payload mass and rope length variation. Meanwhile, the 2-norm of the output weights W_x and W_y are drawn in Fig. 7(b), which are always bounded and finally converge to constant values. Therefore, by updating the prediction model with the online parameter adaptation algorithm (16), the control performance of the proposed anti-swing control method was improved against the parameter uncertainties.

Experiment 3: To evaluate further the control performance and the robustness in harsh operating conditions, the third experiment was conducted by considering the parameter uncertainties and the external disturbances simultaneously. The uncertain parameters were consistent with those in Experiments 1 and 2, and the payload was pushed manually to imitate external disturbances such as accidental collisions. During the experimental process, the amplitudes of the external disturbance occurring at 17 s were approximately $\|\delta\|_{\max} = 0.42$ rad and $\|\theta\|_{\max} = 0.35$ rad. From the results in Fig. 8(a), one can conclude that the proposed method is still robust against both the parameter uncertainties and external disturbances. Moreover, Fig. 8(b) clearly shows that the proposed adaptive predictive anti-swing control can actively interact with the disturbances through the online output weight estimations in the data-driven model.

5. CONCLUSION

An anti-swing control of overhead crane systems has been considered as a challenging control problem due to the high nonlinearity and underactuation in the crane dynamics. Most reported methods for the overhead crane systems utilized physics-based modeling and robust feedback control, which requires broad and significant background knowledge on the underlying physics of the crane system. As a promising alternative solution to the physics-based modeling and control approaches, a novel data-driven modeling scheme and adaptive predictive anti-swing control were proposed in this study. Based on the feedforward neural network and learning scheme called the extreme learning machine, the effective data-driven model of the overhead crane was developed to describe the complex input-output dynamic behaviors. Subsequently, an adaptive predictive anti-swing control law was developed using the obtained data-driven prediction model. In the control scheme, a parameter adaptation law for updating the data-driven model was introduced to the control system to make it more effective in both ordinary and uncertain operating conditions. The stability of the estimation errors and boundedness was analyzed using the Lyapunov method. The extensive experimental results verified that the proposed data-driven modeling and adaptive predictive anti-swing control method were effective for accurate bridge/trolley positioning and payload swing suppressions. Our future work will focus on extending the proposed data-driven modeling and control method to the state constrained control problem of the overhead crane.

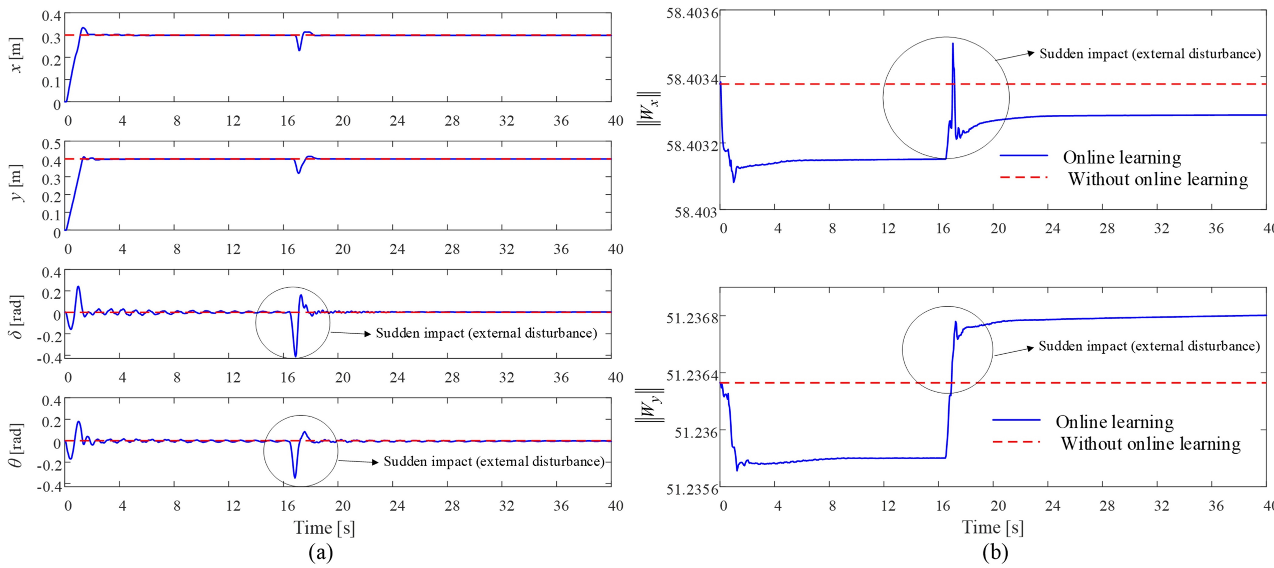

Fig. 8. Experiment 3 – Proposed adaptive predictive anti-swing control in a harsh operating condition: (a) crane responses and (b) online parameter estimation.

REFERENCES

[1] K.-S. Hong and U. H. Shah, *Dynamics and Control of Industrial Cranes*, Springer, Singapore, 2019.

[2] H.-H. Lee, "Motion planning for three-dimensional overhead cranes with high-speed load hoisting," *International Journal of Control*, vol. 78, no. 12, pp. 875-886, 2005.

[3] M. J. Maghsoudi, Z. Mohamed, S. Sudin, S. Buyamin, H. I. Jaafar, and S. M. Ahmad, "An improved input shaping design for an efficient sway control of a nonlinear 3D overhead crane with friction," *Mechanical Systems and Signal Processing*, vol. 92, pp. 364-378, 2017.

[4] P.-T. Pham, G.-H. Kim, Q. C. Nguyen, and K.-S. Hong, "Control of a non-uniform flexible beam: Identification of first two modes," *International Journal of Control, Automation, and Systems*, vol. 19, no. 11, pp. 3698-3707, 2021.

[5] K. L. Sorensen, W. Singhose, and S. Dickerson, "A controller enabling precise positioning and sway reduction in bridge and gantry cranes," *Control Engineering Practice*, vol. 15, no. 7, pp. 825-837, 2007.

[6] A. M. Abdullahi, Z. Mohamed, H. Selamat, H. R. Pota, M. S. Z. Abidin, F. S. Ismail, and A. Haruna, "Adaptive output-based command shaping for sway control of a 3D overhead crane with payload hoisting and wind disturbance," *Mechanical Systems and Signal Processing*, vol. 98, pp. 157-172, 2018.

[7] L. A. Tuan, S.-G. Lee, V.-H. Dang, S. Moon, and B. Kim, "Partial feedback linearization control of a three-dimensional overhead crane," *International Journal of Control, Automation, and Systems*, vol. 11, no. 4, pp. 718-727, 2013.

[8] L. A. Tuan, G.-H. Kim, M. Y. Kim, and S.-G. Lee, "Partial feedback linearization control of overhead cranes with varying cable lengths," *International Journal of Precision Engineering and Manufacturing*, vol. 13, no. 4, pp. 501-507, 2012.

[9] Q. H. Ngo, N. P. Nguyen, Q. B. Truong, and G.-H. Kim, "Application of fuzzy moving sliding surface approach for container cranes," *International Journal of Control, Automation, and Systems*, vol. 19, no. 2, pp. 1133-1138, 2021.

[10] Z. Liu, N. Sun, Y. Wu, and Y. Fang, "Nonlinear sliding mode tracking control of underactuated tower cranes," *International Journal of Control, Automation, and Systems*, vol. 19, no. 2, pp. 1065-1077, 2021.

[11] L. A. Tuan, "Neural observer and adaptive fractional-order backstepping fast-terminal sliding-mode control of RTG cranes," *IEEE Transactions on Industrial Electronics*, vol. 68, no. 1, pp. 434-442, 2021.

[12] G.-H. Kim and K.-S. Hong, "Adaptive sliding mode control of an offshore container crane with unknown disturbances," *IEEE/ASME Transactions on Mechatronics*, vol. 24, no. 6, pp. 2850-2861, 2019.

[13] G.-H. Kim, P.-T. Pham, Q. H. Ngo, and Q. C. Nguyen, "Neural network-based robust anti-sway control of an industrial crane subjected to hoisting dynamics and uncertain hydrodynamic forces," *International Journal of Control, Automation, and Systems*, vol. 19, no. 5, pp. 1953-1961, 2021.

[14] H.-T. Shi, J.-Q. Huang, X. Bai, X. Huang, and J. Sun, "Nonlinear anti-swing control of underactuated tower crane based on improved energy function," *International Journal of Control, Automation, and Systems*, vol. 19, no. 12, pp. 3967-3982, 2021.

[15] P.-Y. Shen, J. Schatz, and R. J. Caverly, "Passivity-based adaptive trajectory control of an underactuated 3-DOF overhead crane," *Control Engineering Practice*, vol. 112, pp. 1-16, 2021.

[16] G.-H. Kim, "Continuous integral sliding mode control of an offshore container crane with input saturation," *International Journal of Control, Automation, and Systems*, vol. 18, no. 9, pp. 2326-2336, 2020.

[17] T. Yang, N. Sun, H. Chen, and Y. Fang, "Neural network-based adaptive antiswing control of an underactuated ship-mounted crane with roll motions and input dead zones," *IEEE Transactions on Neural Networks and Learning Systems*, vol. 31, no. 3, pp. 901-914, 2020.

[18] N. A. Nayfeh and W. T. Baumann, "Nonlinear analysis of time-delay position feedback control of container cranes," *Nonlinear Dynamics*, vol. 53, no. 1, pp. 75-88, 2008.

[19] K.-S. Hong and P.-T. Pham, "Control of axially moving systems: A review," *International Journal of Control, Automation, and Systems*, vol. 17, no. 12, pp. 2983-3008, 2019.

[20] D. Wang, H. He, and D. Liu, "Intelligent optimal control with critic learning for a nonlinear overhead crane system," *IEEE Transactions on Industrial Informatics*, vol. 14, no. 7, pp. 2932-2940, 2017.

[21] H.-H. Lee, "Modeling and control of a three-dimensional overhead crane," *Journal of Dynamic Systems, Measurement, and Control*, vol. 120, no. 4, pp. 471-476, 1998.

[22] B. Lu, Y. Fang, and N. Sun, "Enhanced-coupling adaptive control for double-pendulum overhead cranes with payload hoisting and lowering," *Automatica*, vol. 101, pp. 241-251, 2019.

[23] X. Xing and J. Liu, "PDE modeling and vibration control of overhead crane bridge with unknown control directions and parametric uncertainties," *IET Control Theory and Applications*, vol. 14, no. 1, pp. 116-126, 2019.

[24] B. Lu, Y. Fang, and N. Sun, "Adaptive output-feedback control for dual overhead crane system with enhanced anti-swing performance," *IEEE Transactions on Control Systems Technology*, vol. 28, no. 6, pp. 2235-2248, 2020.

[25] H. Chen, Y. Fang, and N. Sun, "A payload swing suppression guaranteed emergency braking method for overhead crane systems," *Journal of Vibration and Control*, vol. 24, no. 20, pp. 4651-4660, 2018.

[26] H. Chen, Y. Fang, and N. Sun, "A swing constraint guaranteed MPC algorithm for underactuated overhead cranes," *IEEE/ASME Transactions on Mechatronics*, vol. 21, no. 5, pp. 2543-2555, 2016.

[27] L.-H. Lee, C.-H. Huang, S.-C. Ku, Z.-H. Yang, and C.-Y. Chang, "Efficient visual feedback method to control a three-dimensional overhead crane," *IEEE Transactions on Industrial Electronics*, vol. 61, no. 8, pp. 4073-4083, 2014.

[28] T. Yang, N. Sun, and Y. Fang, "Neuroadaptive control for complicated underactuated systems with simultaneous output and velocity constraints exerted on both actuated and unactuated states," *IEEE Transactions on Neural Networks and Learning Systems*, pp. 1-11, 2021. DOI: 10.1109/TNNLS.2021.3115960

[29] T. Yang, H. Chen, N. Sun, and Y. Fang, "Adaptive neural network output feedback control of uncertain underactuated systems with actuated and unactuated state constraints," *IEEE Transactions on Systems, Man, and Cybernetics: Systems*, pp. 1-17, 2021. DOI: 10.1109/TSMC.2021. 3131843

[30] G.-B. Huang, Q.-Y. Zhu, and C.-K. Siew, "Extreme learning machine: Theory and applications," *Neurocomputing*, vol. 70, no. 1-3, pp. 489-501, 2006.

[31] G.-B. Huang, L. Chen, and C.-K. Siew, "Universal approximation using incremental constructive feedforward networks with random hidden nodes," *IEEE Transactions on Neural Networks*, vol. 17, no. 4, pp. 879-892, 2006.

[32] P. Ioannou and J. Sun, *Robust Adaptive Control*, PTR Prentice-Hall, 1996.

[33] J. Spooner, M. Maggiore, R. Ordóñez, and K. Passino, *Stable Adaptive Control and Estimation for Nonlinear Systems: Neural and Fuzzy Approximator Techniques*, Communications and Control Series, Wiley, 2004.

[34] W. H. Kwon and S. Han, *Receding Horizon Control*, Springer-Verlag, New York, 2005.

[35] O. Nelles, *Nonlinear System Identification: From Classical Approaches to Neural Networks and Fuzzy Models*, Springer, 2001.

[36] A. K. Tangirala, *Principles of System Identification: Theory and Practice*, CRC Press, 2014.

[37] L. Ljung, *System Identification: Theory for the User*, Prentice-Hall PTR, New Jersey, 1999.

Gyoung-Hahn Kim received his B.S. degree in mechanical engineering from Yeungnam University, Gyeongsan, in 2013 and a Ph.D. degree in mechanical engineering, Pusan National University, Busan, Korea, in 2021. He is currently a Postdoctoral Fellow in the Institute of Intelligent Logistics and Big Data, Pusan National University. Dr. Kim's current research interests include sliding mode control, adaptive neural network control, reinforcement deep learning, nonlinear system identification, data-driven control, and control applications to industrial robotics.

Mahnjung Yoon received his Master's degree in mechanical part system engineering from Pusan National University, Pusan, in 2010 and completed his doctoral course works in Green Transportation Design System Engineering, Pusan National University, Busan, Korea, in 2017. He is a Managing Director at POWERMnC's Technology Research Center. Mr. Yoon's current research interests include crane boom design, hydraulic precision control, and hoist design as a principal designer of a self-climbing crane for wind power systems.

Jae Young Jeon received his Master's degree in aerospace engineering from the Korea Advanced Institute of Science and Technology (KAIST), Daejeon, in 1985, and his Ph.D. degree in materials engineering, KAIST, Daejeon, Korea, in 1994. He is the CEO at POWERMnC, Ltd. Dr. Jeon's current research interests include developing a self-climbing crane for wind power towers, nuclear fuel handling equipment, and precision measurement equipment for steel plants.

Keum-Shik Hong received his B.S. degree in mechanical design and production engineering from Seoul National University in 1979, his M.S. degree in mechanical engineering from Columbia University, New York, in 1987, and both an M.S. degree in applied mathematics and a Ph.D. degree in mechanical engineering from the University of Illinois at Urbana-Champaign (UIUC) in 1991. He joined the School of Mechanical Engineering at Pusan National University (PNU) in 1993. His Integrated Dynamics and Control Engineering Laboratory was designated a National Research Laboratory by the Ministry of Science and Technology of Korea in 2003. In 2009, under the auspices of the World Class University Program of the Ministry of Education, Science, and Technology (MEST) of Korea, he established the Department of Cogno-Mechatronics Engineering, PNU. He served as Associate Editor of Automatica (2000-2006), as Editor-in-Chief of the Journal of Mechanical Science and Technology (2008-2011), and is serving as the Editor-in-Chief of the International Journal of Control, Automation, and Systems. He was a past President of the Institute of Control, Robotics and Systems (ICROS), Korea, and is President of the Asian Control Association. He was the Organizing Chair of the ICROS-SICE International Joint Conference 2009, Fukuoka, Japan. He is an IEEE Fellow, a Fellow of the Korean Academy of Science and Technology, an ICROS Fellow, a Member of the National Academy of Engineering of Korea, and many other societies. He has received many awards, including the Best Paper Award from the KFSTS of Korea (1999), the F. Harashima Mechatronics Award (2003), the IJCAS Scientific Activity Award (2004), the Automatica Certificate of Outstanding Service (2006), the Presidential Award of Korea (2007), the ICROS Achievement Award (2009), the IJCAS Contribution Award (2010), the Premier Professor Award (2011), the JMST Contribution Award (2011), the IJCAS Contribution Award (2011), the IEEE Academic Award (2016), IJCAS Contribution Award (2020), etc. Dr. Hong's current research interests include brain-computer interface, nonlinear systems theory, adaptive control, distributed parameter systems, autonomous vehicles, and innovative control applications in brain engineering.